Innovative Optically Transparent Planar Antenna for WiMAX Communication Systems

Soukaina Sekkal[1, *], Moustapha El Bakkali[2], Jamal Abounasr[2], Zainab L'Gzouli[1],
Naima Amar Touhami[2], Samoudi Bousselham[1], Adel Asselman[1], and Othmane Bendaou[1]

[1]*Optics, Materials and Systems Team, Abdelmalek Essaadi University, M'Hannech II, B. P. 2121, 93002 Tetouan, Morocco*
[2]*Intelligent Systems Design (ISD) Laboratory, Electronic and Smart Systems (ESS) Team, Faculty of Sciences*
Abdelmalek Essaadi University, Tétouan, Morocco

ABSTRACT: This paper presents a study of a novel optically transparent planar antenna operating at a resonant frequency of 8.5 GHz, specifically designed for WiMAX wireless communication systems. The antenna is fed by a 50 Ω microstrip line and exhibits a wide operational bandwidth. Measuring 30×30 mm^2 and achieving an optical transparency exceeding 70% of glass, the proposed antenna delivers outstanding performance while minimizing its visual impact. It is fabricated using an innovative rectangular meshed pure copper grid layer, deposited on a 0.7-mm-thick borosilicate flat glass substrate, optimizing both transparency and conductivity. Experimental evaluations of key performance parameters, including the reflection coefficient, radiation pattern, and gain, were conducted to assess the antenna's effectiveness at the target frequency of 8.5 GHz. The measured results confirm that the antenna exhibits excellent impedance matching at 8.5 GHz, achieving a peak realized gain of 5.2 dBi. These findings demonstrate the feasibility of transparent antennas that offer performance on par with non-transparent alternatives, while providing distinct aesthetic advantages. As a result, the proposed antenna presents a viable solution for applications requiring both functionality and visual integration, such as smart devices and architectural installations.

1. INTRODUCTION

Antennas play a fundamental role in wireless communication systems, facilitating the transmission and reception of electromagnetic signals between devices. They are essential across a wide range of technologies, including cellular and Wi-Fi networks, satellite communication systems, and navigation devices. Antennas function by converting electrical signals into electromagnetic waves for transmission and vice versa for reception [1]. This enables wireless devices to communicate without physical cables, supporting efficient data transmission over long distances. Furthermore, antennas contribute to improving network performance by enhancing coverage, reducing interference, and optimizing the quality of transmitted or received signals. Modern antenna designs have also evolved to allow seamless integration into electronic devices, promoting compact and efficient designs [2, 3]. In the literature, a wide variety of antenna types have been explored, including rigid, textile, and transparent antennas, each tailored to specific applications and distinguished by its unique features and performance characteristics [4]. Rigid antennas, with their fixed structure and robustness, are typically employed in environments demanding high stability, precision, and reliability, such as in satellite communication systems and industrial applications [5]. Textile antennas, by contrast, are designed for flexibility, lightweight properties, and adaptability, making them ideal for wearable technology and integration into

clothing, where they enable unobtrusive and practical wireless communication. Transparent antennas represent a more recent innovation, offering both aesthetic and functional advantages by combining visual transparency with the capability to transmit and receive electromagnetic signals. These antennas are particularly suited for integration into glass surfaces, electronic displays, or architectural elements, where their ability to maintain visibility and deliver strong communication performance makes them a valuable solution for modern wireless systems [6, 7]. The growing interest in transparent antennas arises from their significant potential for innovative applications across various communication fields, ranging from wireless communication systems to advanced display technologies. These antennas offer the unique advantage of combining functionality with aesthetic appeal, making them ideal for integration into environments where visibility and design considerations are paramount [8, 9]. As a result, substantial research efforts have been dedicated to developing and optimizing transparent antenna technologies [10–12]. The functionality of transparent antennas relies on the use of materials that are both conductive and optically transparent for the radiating elements, along with fully transparent dielectric substrates. Transparent Conductive Materials (TCMs) are fundamental to these designs, offering a critical balance between high electrical conductivity and excellent optical transparency. Beyond their conductive properties, TCMs exhibit robustness, mechanical flexibility, and environmental stability, which are essential for their deployment in a wide range of applications [13].

---

* Corresponding author: Soukaina Sekkal (sekkalsoukaina92@gmail.com).

These versatile materials have attracted considerable attention in the development of optically transparent electronic components. Their properties make them invaluable not only for transparent antennas but also for advanced technologies such as optical antennas [14], organic light-emitting diodes (OLEDs) [15], liquid crystal displays (LCDs) [16], and solar cells [17]. In these applications, TCMs facilitate the seamless integration of transparency and functionality, enabling the creation of devices that are both visually unobtrusive and highly efficient. The ongoing advancements in transparent conductive materials and their application in antenna design signal a promising future for this technology [18]. Researchers continue to explore novel material combinations, improved fabrication techniques, and innovative designs to enhance the performance, efficiency, and durability of transparent antennas, ensuring their suitability for an ever-expanding range of cutting-edge applications [19]. Among the most widely used Transparent Conductive Materials (TCMs) are transparent conductive films and metal meshes. Transparent conductive films, such as fluorine-doped tin oxide (FTO) [20], silver polymer (AgHT) [12], and indium tin oxide (ITO) [21], are valued for their high transparency and lightweight properties. These characteristics make them suitable for applications where minimizing visual and physical impact is crucial. However, antennas fabricated from these films often suffer from lower gains and reduced radiation efficiency compared to their metal-based counterparts, primarily due to the inherent limitations of these materials in conducting electricity effectively over large areas. In contrast, antennas designed using metal meshes have shown substantial improvements in efficiency and radiation gain, owing to the superior conductivity of their metallic structures. The metallic composition of these meshes allows for better electrical performance while still maintaining a degree of optical transparency, as evidenced by studies in [22–24]. This makes metal meshes an increasingly popular choice for applications requiring a balance between performance and aesthetics. The fabrication of fully transparent antennas typically involves depositing these conductive, transparent materials onto equally transparent substrates, such as specialized plastics or glass films [25, 26]. This process ensures that the antennas preserve their optical transparency without compromising their electrical functionality. By leveraging advanced materials and fabrication techniques, transparent antennas can achieve the dual goals of high performance and visual integration, paving the way for their adoption in a wide range of modern applications [27]. Although 8.5 GHz is not a standard frequency for WiMAX, it lies within a broader frequency range considered for future extensions of WiMAX and similar wireless technologies. The IEEE 802.16 standard, which defines the operational parameters for WiMAX, recognizes frequencies below 11 GHz — such as 8.5 GHz — as potential candidates for both Line-of-Sight (LOS) and Non-Line-of-Sight (NLOS) communication in future wireless systems. Positioned in the mid-band spectrum, 8.5 GHz is particularly important for the development of next-generation communication technologies, including 5G and future iterations of WiMAX, due to its ability to support high-capacity, low-latency transmission. Furthermore, several studies have shown the feasibility of operating antennas at 8.5 GHz, confirming its suit-

ability for high-performance wireless communication systems [28]. This underscores the growing importance of 8.5 GHz in the context of emerging high-speed, high-capacity wireless networks.

This paper presents the design and fabrication of a planar antenna characterized by its transparency and near invisibility, specifically designed for wireless communication systems operating in the microwave band, such as WiMAX. The proposed antenna is developed using an innovative rectangular copper mesh structure deposited onto a transparent glass substrate, carefully selected to balance optical clarity and structural durability. This innovative approach enables the creation of an antenna that is both visually unobtrusive and highly transparent, making it suitable for the integration into applications where aesthetic considerations are critical, such as modern architectural designs, electronic displays, and automotive systems. In addition to its transparency, the proposed antenna demonstrates optimal electrical conductivity and robust performance, meeting the stringent requirements of microwave communication systems. The choice of materials and design methodology ensure a balance between visual invisibility and high radiation efficiency, providing a practical solution for next-generation wireless communication systems that demand minimal visual impact without compromising functionality. The remainder of the paper is organized as follows. Section 1 provides an in-depth description of the materials chosen for the dielectric and conductive components of the proposed transparent antenna. It also details the design methodology, including the determination of specific dimensions to optimize performance. Section 2 focuses on evaluating the performance of the transparent antenna within wireless communication systems, particularly for WiMAX applications. This evaluation includes both simulation and experimental measurement results, with a detailed analysis of key performance metrics such as the reflection coefficient (S_{11}) and antenna gain to validate the effectiveness of the proposed design.

2. MATERIALS AND METHODS

2.1. Material Selection for Transparent Antenna Design

Choosing the right material is a critical factor in antenna design, as it directly influences the antenna's performance, durability, and suitability for specific applications. For transparent antennas, the material must offer a unique combination of optical transparency, electrical conductivity, mechanical flexibility, and environmental resilience. These properties are essential to ensure that the antenna can maintain high efficiency while blending seamlessly into its environment, particularly for applications where aesthetics and visibility are key considerations. With these requirements in mind, the fine copper mesh used in this study was carefully selected as the conductive material due to its superior electrical performance, flexibility, and compatibility with transparent substrates. The proposed transparent antenna consists of two parts: a conductive layer for signal transmission and reception and a non-conductive dielectric substrate for structural support and optical transparency. This dual-component design balances mechanical stability with electrical

performance, ensuring efficiency and invisibility. The conductive part is an innovative rectangular fine copper mesh, while the substrate is a transparent borosilicate material.

In the proposed antenna design, the conductive component is implemented using a fine copper mesh, selected for its excellent electrical conductivity, mechanical flexibility, and compatibility with transparent substrates. Figure 1(a) depicts this innovative fine copper mesh, manufactured by The Mesh Company, which integrates structural precision with advanced material properties. The mesh is meticulously woven from solid copper wires, forming a uniform rectangular grid, with each unit measuring 0.408 mm in length. This precise and consistent design ensures both functionality and structural homogeneity, making it an ideal choice for high-performance transparent antenna applications. The mesh exhibits a uniform spacing of 0.204 mm between the copper strips and a thickness of 0.05 mm, ensuring dimensional homogeneity, flexibility, and lightweight characteristics. This unique configuration enables the passage of visible light, making the mesh highly suitable for applications such as Radio Frequency Interference (RFI) and Electromagnetic Interference (EMI) shielding. The copper material provides exceptional electrical conductivity and surpasses stainless steel alternatives in ease of handling, flexibility, and integration into complex designs. These qualities make the mesh a compelling choice for modern antenna applications, where high performance and aesthetic transparency are critical. Additionally, the mesh is corrosion-resistant, ensuring durability and reliability under various environmental conditions. Figure 1(b) shows the side view of the Metal Mesh Film (MMF) structure. To protect the delicate copper strips, which are only 0.05 mm thick, the mesh is mounted on a transparent borosilicate substrate, as shown in Figure 1(c). In the simulation model, the borosilicate glass substrate was characterized using a relative permittivity $\varepsilon_r = 4.4$ and a loss tangent $\tan \delta = 0.0058$. These values were chosen based on standard data for borosilicate materials and were used to ensure accurate electromagnetic modeling of the antenna's performance. This substrate enhances structural stability while maintaining optical transparency, making the design suitable for advanced wireless systems requiring both functional efficiency and visual integration. The thicknesses of the strip lines and borosilicate glass substrate are t and h, respectively.
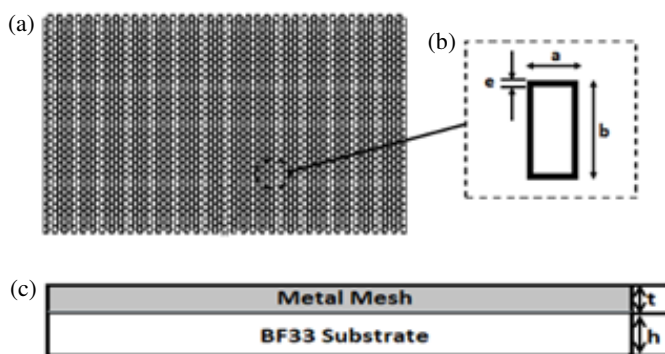

FIGURE 1. Structure of the Metal Mesh Film (MMF): (a) front view, (b) unit cell, and (c) side view.

2.2. Proposed Transparent Antenna Design

The design of the antenna is based on fundamental principles of antenna theory, including electromagnetic radiation, material conductivity, and the effects of materials used. Antenna radiation is analyzed using the Friis transmission equation, which helps determine antenna gain and efficiency [29].

$$G = \frac{4\pi A_e}{\lambda^2} \tag{1}$$

where G is the antenna gain, A_e the effective area, and λ the wavelength. The conductivity of copper, used in the design of the mesh grid, reduces ohmic losses, and the antenna's impedance can be calculated as [11]:

$$W = \sqrt{\frac{L}{C}} \tag{2}$$

where L is the inductance, and C is the capacitance of the antenna circuit. The borosilicate glass substrate used in the design provides a low loss factor, ensuring both optical transparency and high efficiency at the target frequency.

In designing the proposed transparent antenna, several technical aspects were carefully considered to ensure optimal performance at the target operating frequency of 8.5 GHz, while balancing the aesthetic and functional requirements of modern applications. Using advanced Computer Simulation Technology (CST) Microwave Studio simulation software, the antenna geometry and material properties were carefully optimized to ensure efficient radiation and stable performance at this resonant frequency. Parameters such as the overall width and length of the copper mesh strips, constituting the conductive part of the patch and the ground plane, were precisely adjusted to achieve this goal, while maintaining good impedance compatibility and a compact and lightweight profile suitable for integration into portable and fixed devices. The parameters of the proposed transparent antenna are shown in Figure 2, which illustrates in detail the geometric dimensions and structural layout required to ensure its optimal performance. These parameters include the precise dimensions of the copper conductive mesh, which define the characteristics of the patch, as well as the overall size of the borosilicate glass substrate. They also include the properties of the feedline, including its length and width, as well as the dimensions of the ground plane. All these parameters have been carefully optimized to ensure good impedance matching and efficient radiation, while maintaining a balance between compactness, lightness, and functional efficiency, thus meeting the aesthetic and technical requirements of the antenna.

All these parameters have been carefully selected and optimized to ensure good impedance matching and efficient radiation at the resonance at the target frequency of 8.5 GHz, while maintaining the desired optical transparency, mechanical robustness, and electrical efficiency. The precise alignment of these parameters ensures that the antenna operates efficiently in the microwave frequency band, making it suitable for applications requiring both high performance and aesthetic integration. Figure 2 provides a comprehensive visual representation of these key design aspects, offering insight into the structural
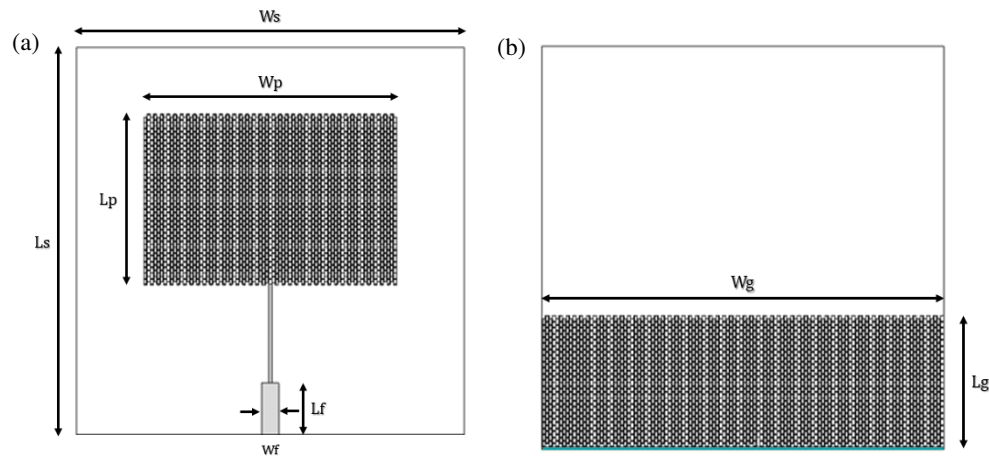
FIGURE 2. Geometry of the transparent patch antenna: (a) front view, (b) back view.

and functional elements of the proposed antenna. To complement the visual representation in Figure 2, Table 1 presents the antenna parameters' specific values in detail. This table provides a clear and concise overview of the design dimensions and material properties, offering a complete understanding of the proposed antenna's structure. Table 1 presents the dimensions of the key elements in the antenna design. Parameters W_s and L_S refer to the width and length of the substrate, respectively, which is made of borosilicate glass. Dimensions W_P and L_P represent the width and length of the patch, which is fabricated from a copper mesh grid. Parameters W_g and L_g correspond to the ground plane dimensions, where W_g is the width, and L_g is the length, which are critical for ensuring good impedance matching and optimal performance. Finally, W_f and L_f represent the width and length of the feedline, which is used to deliver the signal to the antenna.

TABLE 1. Design parameters and their values.

Parameters	W_S	L_S	W_P	L_P	W_g	L_g	W_f	L_f
Values (mm)	30	30	23	14	30	10	1.3	4

A parametric analysis was conducted to study the effect of the feedline length (L_f) on the antenna's reflection coefficient (S_{11}). As shown in Figure 3, increasing L_f from 1 mm to 4 mm results in a noticeable shift in the resonant frequency. Specifically, when $L_f = 4$ mm, the resonant frequency moves close to 9.0 GHz, deviating from the desired 8.5 GHz operating point. Among the tested values, $L_f = 3$ mm provides the best impedance matching at a resonance near 8.5 GHz, with an S_{11} below -25 dB, making it the most suitable configuration for WiMAX applications. This parametric study confirms that the feedline length significantly affects the input impedance and resonance behavior of the antenna. In addition to L_f, we performed further parametric studies on other antenna parameters (not shown here) to finely adjust the overall design and achieve optimal performance at 8.5 GHz. The combination of these optimizations allowed us to precisely tune the antenna's frequency response to meet the target specification.
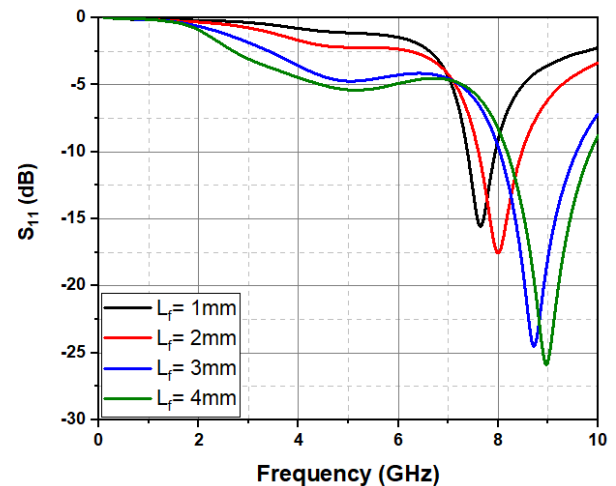

FIGURE 3. Effect of feedline length (L_f) on the reflection coefficient (S_{11}) of the proposed transparent antenna.

3. RESULTS AND PERFORMANCE ANALYSIS

3.1. Assessment of Simulated and Measured S_{11} Performance

To evaluate the performance of the proposed transparent antenna, both simulation and experimental measurements were conducted. Simulations were carried out using CST Microwave Studio to analyze the antenna's electromagnetic behavior and optimize its design parameters for resonance at 8.5 GHz. The experimental testing was performed in a controlled laboratory environment using a Vector Network Analyzer (VNA) Rohde schwarz-ZVB20 to measure key performance metrics, including the reflection coefficient S_{11} and radiation pattern. The testing setup was designed to replicate real-world conditions while minimizing external interference, ensuring accurate and reliable measurements.

The results include a detailed comparison of the simulated and measured S_{11} and radiation patterns, highlighting the antenna's ability to achieve effective impedance matching at the target frequency. These results validate the design approach, demonstrating that the proposed antenna performs well in terms of resonance, radiation efficiency, and return loss. The agree-
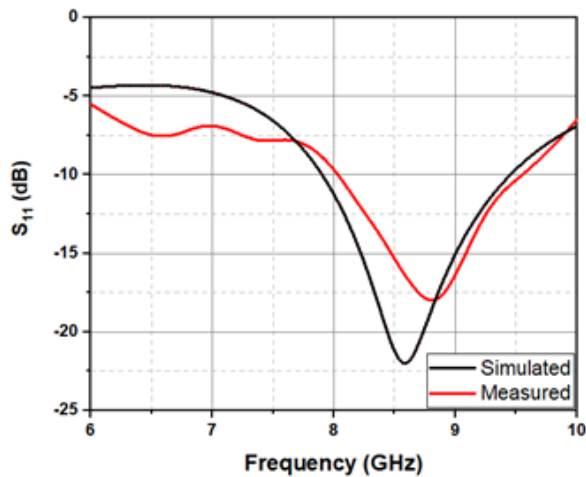
FIGURE 4. Simulated and measured reflection coefficients of the transparent patch antenna.

FIGURE 5. Simulated and measured gains.

ment between the simulation and measurement data confirms the antenna's suitability for transparent and high-performance wireless applications. The following sections provide an in-depth presentation and analysis of these results, emphasizing the antenna's practical performance in achieving the desired transparency and functionality.

Figure 4 shows the simulated and measured reflection coefficients (S_{11}) of the proposed optically transparent planar antenna. The antenna achieves good impedance matching at the resonant frequency of 8.5 GHz, where the reflection coefficient reaches a minimum of approximately -23 dB in the simulation and -18 dB in the measurement. Based on the measured reflection coefficient, the antenna demonstrates a -10 dB impedance bandwidth of approximately 1.45 GHz, covering the frequency range from 8.10 GHz to 9.55 GHz. This wide bandwidth encompasses the 8.5 GHz WiMAX band (IEEE 802.16e), ensuring that the proposed antenna is well suited for broadband wireless access applications. The wideband behavior also provides flexibility for the use in adjacent high-frequency communication bands. The difference between simulation and measurement can be further explored by considering factors like material tolerances, fabrication imperfections, and experimental conditions. Variations in copper conductivity, borosilicate glass loss, dimensional inaccuracies, misalignment, and environmental factors can all contribute to discrepancies. Despite these differences, the overall agreement between the measured and simulated results remains satisfactory, confirming the validity of the antenna design.

The close agreement between the measured and simulated results validates the antenna's design methodology, material selection, and fabrication process. This also demonstrates the feasibility of using a rectangular meshed pure copper grid layer deposited on a borosilicate glass substrate for optically transparent antennas. The achieved performance, combined with the antenna's aesthetic advantages, makes it a strong candidate for applications requiring both visual transparency and high-frequency operation.
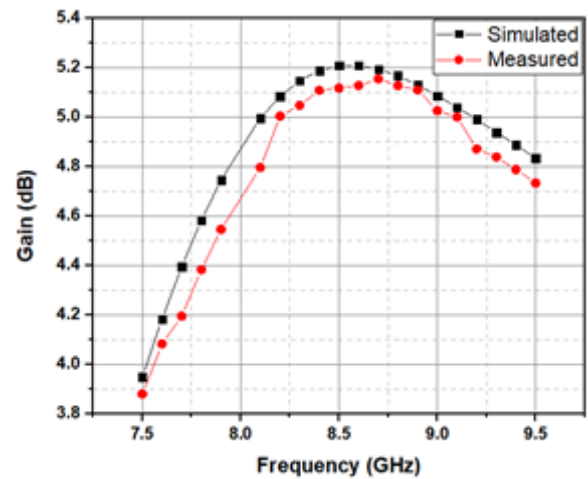
3.2. Evaluation of Gain and Radiation Pattern Characteristics

Figure 5 compares the simulated and measured gains of the proposed optically transparent planar antenna across a frequency range of 7.5 GHz to 9.5 GHz. Both curves exhibit a similar trend, with the gain peaking near 8.5 GHz at approximately 5.2 dB. The measured gain is slightly lower than the simulated gain, likely due to practical factors such as material losses or imperfections in fabrication and measurement setup. The gain is calculated using the Friis transmission equation, and measurements are repeated across the frequency range to evaluate performance. This process ensures accurate characterization of the antenna's directional efficiency and performance.

In addition, a 3D radiation pattern of the antenna at 8.5 GHz is presented in Figure 6. The plot confirms that the antenna exhibits a directional radiation characteristic, with the majority of the radiated energy concentrated in the main lobe. The maximum realized gain reaches approximately 5.35 dBi, validating the antenna's efficiency in transmitting energy in a specific di-
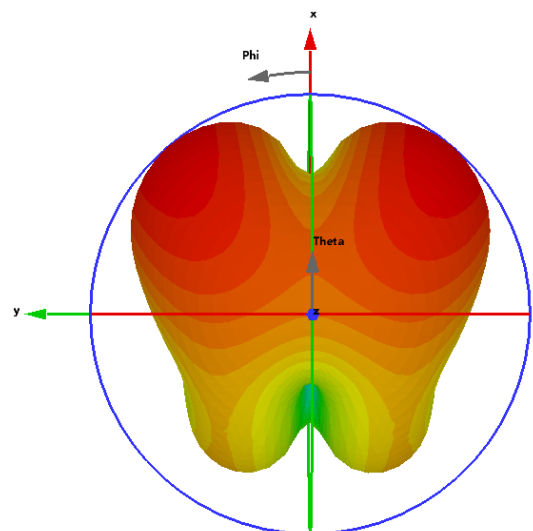

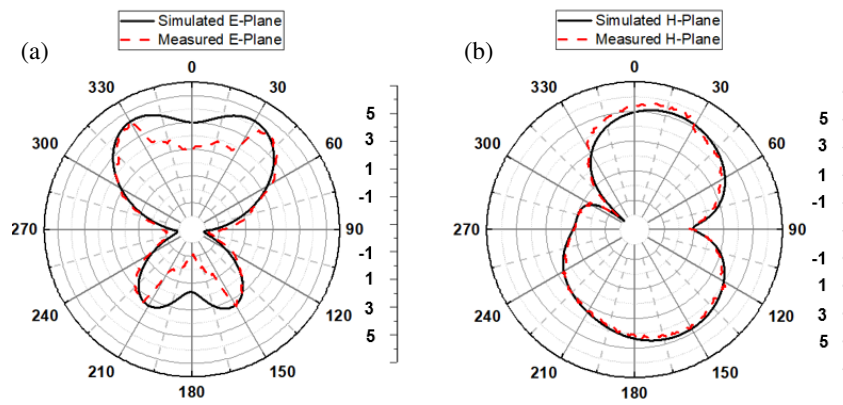FIGURE 6. 3D radiation pattern of the proposed transparent antenna at 8.5 GHz.

FIGURE 7. Simulated and measured radiation patterns: (a) E-Plane, (b) H-Plane.

TABLE 2. Comparison of transparent antennas.

Antenna Design	Dimensions (mm³)	Substrate Material	Bandwidth (%)	Peak Gain (dBi)	Efficiency (%)	Transparency (%)	Reference
Transparent Dual-Band Antenna	$35 \times 35 \times 1.84$	Glass (Plexiglas)	13.27, 5.28	0.70, 1.67	85.5	92	[30]
Dual-Band Optically Transparent Antenna	$50 \times 50 \times 1.48$	Glass (Plexiglas)	9.16, 21.98	2.26, 2.11	88	94	[31]
Transparent Monopole Antenna	$90 \times 60 \times 2$	Glass	41.89	3.16	90	90	[32]
Dual Band Transparent and Nontransparent Antennas for Wireless Application	$30 \times 30 \times 2$	Glass	9.71, 3.81	3.2	92	91	[33]
Miniaturized Wearable Button Antenna for Wi-Fi and Wi-Max	$10 \times 10 \times 2$	Acrylic Sheet	10.9	< 1.38	80	98	[34]
The Proposed Antenna	$30 \times 30 \times 1.5$	**BF33**	**17.64**	**5.2**	**95**	**92**	**This Work**

rection. Regions of lower gain indicate reduced radiation intensity, consistent with directional antenna behavior. This makes the proposed design well suited for point-to-point communication links and WiMAX systems where high directivity and efficient coverage are essential.

Furthermore, the surface current distribution at 8.5 GHz is illustrated in Figure 9, highlighting how the current flows across the antenna structure. The color scale indicates the current magnitude (in V/m), while arrows denote the direction of current flow. The strongest currents, shown in red, are concentrated along the central and edge regions of the copper mesh, confirming that these parts play a dominant role in the radiation process. The overall uniform distribution of surface current supports efficient radiation at the resonant frequency, aligning with the antenna's measured gain and S_{11} characteristics. Areas

of minimal current, mainly away from the radiating structure, further reinforce the directional and well-confined behavior of the design.

The measurement setup to assess the characteristics of the radiation pattern is depicted in Figure 8. The experimental configuration includes the antenna under test, a transmitting antenna mounted on a tripod, and the necessary alignment for precise measurement. This setup ensures the accurate and reliable characterization of radiation properties across the operational frequency range. The radiation pattern evaluation, presented in Figure 7, is conducted in both the E-plane and H-plane, showing a strong correlation between simulated and measured results, with minor discrepancies due to fabrication tolerances and measurement conditions. The E-plane exhibits a characteristic butterfly-shaped pattern, while the H-plane shows a more
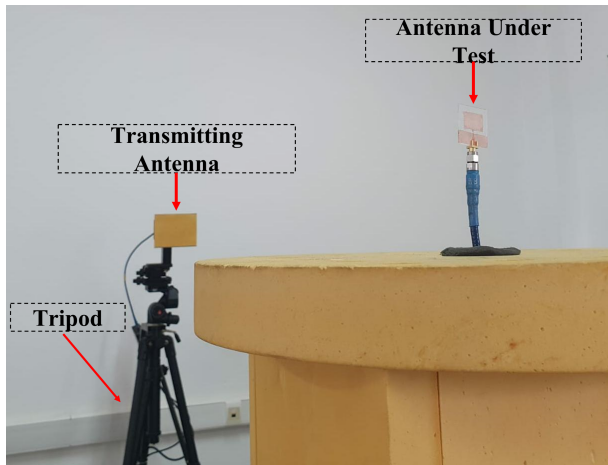
FIGURE 8. Experimental setup for measuring the radiation pattern of the proposed antenna.

FIGURE 9. Surface current distribution of the proposed antenna at 8.5 GHz.

uniform, bi-directional distribution, confirming the expected antenna behavior. The measured results closely follow the simulated patterns, validating the accuracy of the design and its predicted performance. Small variations may arise due to environmental factors, feeding alignment, or material inconsistencies, but overall, the antenna exhibits stable radiation properties with well-defined lobes and nulls, ensuring its effectiveness for the intended wireless communication application.

4. DISCUSSION

Table 2 presents a comparative analysis of the proposed optically transparent planar antenna with other state-of-the-art transparent antenna designs. The comparison considers key parameters such as antenna dimensions, substrate material, bandwidth, and peak gain. The proposed antenna, designed on a BF33 glass substrate with compact dimensions of $30 \times 30 \times 1.5\,\mathrm{mm}^3$, achieves a bandwidth of 5.2 MHz, making it suitable for WiMAX communication systems. Compared to existing designs, it offers a balance between compactness and operational efficiency while ensuring optical transparency. The observed variations in bandwidth and gain across different designs can be attributed to differences in substrate materials, fabrication techniques, and antenna geometries. The results demonstrate that the proposed antenna provides competitive performance with enhanced miniaturization, making it a viable candidate for transparent and wearable wireless applications.

5. CONCLUSION

In this study, an optically transparent planar antenna was designed to offer an excellent compromise between performance and aesthetics, resonating at 8.5 GHz. This performance was achieved thanks to an innovative design integrating a pure copper grid layer with rectangular meshes, deposited on a borosilicate glass substrate. This grid plays a crucial role in optimizing the antenna characteristics, in particular by allowing a
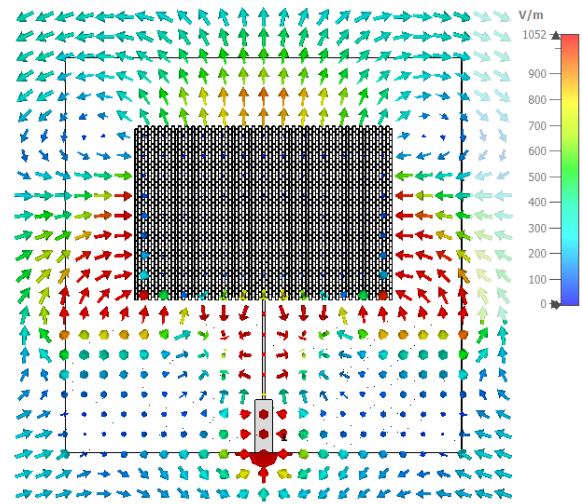
good compromise between optical transparency and conductivity. The antenna achieves a maximum gain of 5.2 dBi and a bandwidth suitable for WiMAX wireless communication systems, demonstrating its ability to meet the technical requirements of these systems while remaining discreet. The experimental results confirm the feasibility of integrating transparent antennas in applications requiring high technical performance and minimal visual impact. This design enables the antenna to be used in environments where discretion is essential, while maintaining performance characteristics comparable to those of non-transparent antennas. These results open the way to innovative solutions for discreet external antennas, thus offering significant potential for applications in devices or infrastructures where aesthetics and functionality must be combined.

REFERENCES

[1] Balanis, C. A., "Antenna theory: A review," *Proceedings of the IEEE*, Vol. 80, No. 1, 7–23, 2002.

[2] Lo, Y. T. and S. W. Lee, *Antenna Handbook: Theory, Applications, and Design*, Springer Science & Business Media, 2013.

[3] Jain, P., P. K. Sahoo, A. D. Khaleel, and A. J. A. Al-Gburi, "Enhanced prediction of metamaterial antenna parameters using advanced machine learning regression models," *Progress In Electromagnetics Research C*, Vol. 146, 1–12, 2024.

[4] Kirtania, S. G., A. W. Elger, M. R. Hasan, A. Wisniewska, K. Sekhar, T. Karacolak, and P. K. Sekhar, "Flexible antennas: A review," *Micromachines*, Vol. 11, No. 9, 847, 2020.

[5] El Misilmani, H. M., M. Al-Husseini, K. Y. Kabalan, and A. El-Hajj, "A simple miniaturized triple-band antenna for WLAN/WiMAX applications," in *PIERS Proceedings*, 608–612, Moscow, Russia, Aug. 2012.

[6] Sayem, A. S. M., A. Lalbakhsh, K. P. Esselle, J. L. Buckley, B. O'Flynn, and R. B. V. B. Simorangkir, "Flexible transparent antennas: Advancements, challenges, and prospects," *IEEE Open Journal of Antennas and Propagation*, Vol. 3, 1109–1133, 2022.

[7] Soni, G. K., D. Yadav, A. Kumar, P. Jain, and A. Rathi, "Design and SAR analysis of DGS based deformed microstrip antenna for ON/OFF body smart wearable IoT applications," *Physica Scripta*, Vol. 100, No. 1, 015536, 2024.

[8] Green, R. B., M. Guzman, N. Izyumskaya, B. Ullah, S. Hia, J. Pitchford, R. Timsina, V. Avrutin, U. Ozgur, H. Morkoc, N. Dhar, and E. Topsakal, "Optically transparent antennas and filters: A smart city concept to alleviate infrastructure and network capacity challenges," *IEEE Antennas and Propagation Magazine*, Vol. 61, No. 3, 37–47, 2019.

[9] Soni, G. K., D. Yadav, A. Kumar, P. Jain, and M. V. Yadav, "Design and optimization of flexible DGS-based microstrip antenna for wearable devices in the Sub-6 GHz range using the nelder-mead simplex algorithm," *Results in Engineering*, Vol. 24, 103470, 2024.

[10] El Halaoui, M., A. Kaabal, H. Asselman, S. Ahyoud, and A. Asselman, "Multiband planar inverted-F antenna with independent operating bands control for mobile handset applications," *International Journal of Antennas and Propagation*, Vol. 2017, No. 1, 8794039, 2017.

[11] Haraty, M. R., M. Naser-Moghadasi, A. A. Lotfi-Neyestanak, and A. Nikfarjam, "Improving the efficiency of transparent antenna using gold nanolayer deposition," *IEEE Antennas and Wireless Propagation Letters*, Vol. 15, 4–7, 2015.

[12] Desai, A., T. Upadhyaya, and R. Patel, "Compact wideband transparent antenna for 5G communication systems," *Microwave and Optical Technology Letters*, Vol. 61, No. 3, 781–786, 2019.

[13] Sissoko, A., C. O. Sanogo, and B. Diourté, "A review on conductive and transparent materials used in the design of transparent antennas," *Open Journal of Antennas and Propagation*, Vol. 11, No. 2, 11–25, 2023.

[14] Lim, E. H. and K. W. Leung, "Transparent dielectric resonator antennas for optical applications," *IEEE Transactions on Antennas and Propagation*, Vol. 58, No. 4, 1054–1059, 2010.

[15] Zhang, D., K. Ryu, X. Liu, E. Polikarpov, J. Ly, M. E. Thompson, and C. Zhou, "Transparent, conductive, and flexible carbon nanotube films and their application in organic light-emitting diodes," *Nano Letters*, Vol. 6, No. 9, 1880–1886, 2006.

[16] Ting, T.-L., "Technology of liquid crystal based antenna," *Optics Express*, Vol. 27, No. 12, 17138–17153, 2019.

[17] Varghese, O. K., M. Paulose, and C. A. Grimes, "Long vertically aligned titania nanotubes on transparent conducting oxide for highly efficient solar cells," *Nature Nanotechnology*, Vol. 4, No. 9, 592–597, 2009.

[18] Chishti, A. R., A. Aziz, M. A. Qureshi, M. N. Abbasi, A. M. Algarni, A. Zerguine, N. Hussain, and R. Hussain, "Optically transparent antennas: A review of the state-of-the-art, innovative solutions and future trends," *Applied Sciences*, Vol. 13, No. 1, 210, 2022.

[19] Soni, G. K., D. Yadav, and A. Kumar, "Design consideration and recent developments in flexible, transparent and wearable antenna technology: A review," *Transactions on Emerging Telecommunications Technologies*, Vol. 35, No. 1, e4894, 2024.

[20] Peter, T., T. A. Rahman, S. W. Cheung, R. Nilavalan, H. F. Abutarboush, and A. Vilches, "A novel transparent UWB antenna for photovoltaic solar panel integration and RF energy harvesting," *IEEE Transactions on Antennas and Propagation*, Vol. 62, No. 4, 1844–1853, 2014.

[21] Colombel, F., X. Castel, M. Himdi, G. Legeay, S. Vigneron, and E. M. Cruz, "Ultrathin metal layer, ITO film and ITO/Cu/ITO multilayer towards transparent antenna," *IET Science, Measurement & Technology*, Vol. 3, No. 3, 229–234, 2009.

[22] Turpin, T. W. and R. Baktur, "Meshed patch antennas integrated on solar cells," *IEEE Antennas and Wireless Propagation Letters*, Vol. 8, 693–696, 2009.

[23] Clasen, G. and R. Langley, "Meshed patch antennas," *IEEE Transactions on Antennas and Propagation*, Vol. 52, No. 6, 1412–1416, 2004.

[24] Hautcoeur, J., L. Talbi, K. Hettak, and M. Nedil, "60 GHz optically transparent microstrip antenna made of meshed AuGL material," *IET Microwaves, Antennas & Propagation*, Vol. 8, No. 13, 1091–1096, 2014.

[25] Hussain, M., H. Zahra, S. M. Abbas, and Y. Zhu, "Flexible dielectric materials: potential and applications in antennas and RF sensors," *Advanced Electronic Materials*, Vol. 10, No. 11, 2400240, 2024.

[26] El Gharbi, M., R. Fernández-García, S. Ahyoud, and I. Gil, "A review of flexible wearable antenna sensors: Design, fabrication methods, and applications," *Materials*, Vol. 13, No. 17, 3781, 2020.

[27] Tong, C., *Advanced Materials for Printed Flexible Electronics*, Springer, 2022.

[28] Baabdullah, F., A. Affandi, and A. M. Dobaie, "Design microstrip patch antenna for WiMAX applications at 8.5 GHz," *Simulation*, Vol. 3, 39–2, 2016.

[29] Balanis, C. A., *Antenna Theory: Analysis and Design*, John Wiley & Sons, 2015.

[30] Desai, A. and T. Upadhyaya, "Transparent dual band antenna with μ-negative material loading for smart devices," *Microwave and Optical Technology Letters*, Vol. 60, No. 11, 2805–2811, 2018.

[31] Desai, A., T. Upadhyaya, M. Palandoken, R. Patel, and U. Patel, "Dual band optically transparent antenna for wireless applications," in *2017 IEEE Asia Pacific Microwave Conference (APMC)*, 960–963, Kuala Lumpur, Malaysia, 2017.

[32] Azini, A. S., M. R. Kamarudin, T. B. A. Rahman, H. U. Iddi, A. Y. Abdulrahman, and M. F. B. Jamlos, "Transparent antenna design for WiMAX application," *Progress In Electromagnetics Research*, Vol. 138, 133–141, 2013.

[33] Desai, A. H. and T. Upadhyaya, "Dual-band transparent and non-transparent antennas for wireless application," *International Journal of Electronics Letters*, Vol. 8, No. 2, 170–179, 2020.

[34] Mandal, B. and S. K. Parui, "A miniaturized wearable button antenna for Wi-Fi and Wi-Max application using transparent acrylic sheet as substrate," *Microwave and Optical Technology Letters*, Vol. 57, No. 1, 45–49, 2015.